

Electronic supplementary information

Facile and green synthesis of hydrophilic imprinted resin in deep eutectic solvents-water for specific molecular recognition of tumor biomarkers in complex biological matrices

Mingwei Wang^a, Liang Zhou^a, Fengxia Qiao^c, Hongyuan Yan^{a,b*}

^a Hebei Key Laboratory of Public Health Safety, College of Pharmaceutical Science, College of

Chemistry and Materials Science, Hebei University, Baoding 071002, China

^b State Key Laboratory of New Pharmaceutical Preparations and Excipients, Key Laboratory of

Medicinal Chemistry and Molecular Diagnosis of Ministry of Education, Hebei University,

Baoding 071002, China

^c College of Biochemical and Environmental Engineering, Baoding University, Baoding,

071002, China

* Corresponding author. Tel./Fax: +86-312-5079788

E-mail address: yanhy@hbu.edu.cn

Contents

Chemicals and reagents

Characterization and analysis instruments

Adsorption experiments

Adsorption kinetics

Adsorption isotherms

Urine sample pretreatment procedure

Figures and Tables

Fig. S1 Fourier-transform infrared spectroscopy (FTIR) spectra of HIR and HNIR.

Fig. S2 Pseudo-first-order (a) and Pseudo-second-order (b) kinetics models of HIR for adsorption of VMA and HVA.

Fig. S3 Pseudo-first-order (a) and Pseudo-second-order (b) kinetics models of HNIR for adsorption of VMA and HVA.

Fig. S4 Adsorption isotherm models of HIR for adsorption of VMA and HVA at different temperatures. (a) Langmuir linear fits for VMA; (b) Langmuir linear fits for HVA; (c) Freundlich linear fits for VMA; (d) Freundlich linear fits for HVA; (e) Tempkin linear fits for VMA; (f) Tempkin linear fits for HVA; (g) D - R linear fits for VMA; (h) D - R linear fits for HVA.

Fig. S5 Adsorption isotherm models of HNIR for adsorption of VMA and HVA at different temperatures. (a) Langmuir linear fits for VMA; (b) Langmuir linear fits for HVA; (c) Freundlich linear fits for VMA; (d) Freundlich linear fits for HVA; (e)

Tempkin linear fits for VMA; (f) Tempkin linear fits for HVA; (g) D - R linear fits for VMA; (h) D - R linear fits for HVA.

Fig. S6 The plots of $\ln K_f$ versus $1/T$ for VMA and HVA of HIR (a) and HNIR (b).

Fig. S7 High-resolution XPS spectra of HIR before adsorption of VMA, HVA (a) C1s, (b) O1s and after adsorption of VMA, HVA (c) C1s, (d) O1s.

Fig. S8 Effect factors of separation and extraction conditions study. (a) pH; (b) salt concentration; (c) adsorbent amount; (d) the kind of washing solvent (1.methanol; 2.acetonitrile; 3.acetone; 4.water; 5.methanol-water (1:1, v/v); 6.acetonitrile-water (1:1, v/v)); (e) the volume of washing solvent; (f) the kind of eluent (1.methanol-acetic acid (9:1, v/v); 2.methanol-formic acid (9:1, v/v); 3.acetonitrile-acetic acid (9:1, v/v); 4.acetonitrile-formic acid (9:1, v/v); 5.acetonitrile-ammonia water (9:1, v/v); 6.methanol-ammonia water (9:1, v/v)); (g) the volume of eluent).

Table S1. Lagergren pseudo-first-order and pseudo-second-order kinetics parameters of HIR for the adsorption of VMA and HVA.

Table S2. Lagergren pseudo-first-order and pseudo-second-order kinetics parameters of HNIR for the adsorption of VMA and HVA.

Table S3. Langmuir isotherm for the adsorption of analytes on HIR.

Table S4. Langmuir isotherm for the adsorption of analytes on HNIR.

Table S5. Freundlich isotherm for the adsorption of analytes on HIR.

Table S6. Freundlich isotherm for the adsorption of analytes on HNIR.

Table S7. Tempkin isotherm for the adsorption of analytes on HIR.

Table S8. Tempkin isotherm for the adsorption of analytes on HNIR.

Table S9. D-R isotherm for the adsorption of analytes on HIR.

Table S10. D-R isotherm for the adsorption of analytes on HNIR.

Table S11. Thermodynamics parameters for the adsorption of analytes on HIR.

Table S12. Thermodynamics parameters for the adsorption of analytes on HNIR.

Table S13. Methodology parameters of the HIR-SPE-HPLC.

Table S14. Spiked recovery of the HIR-SPE-HPLC method.

Table S15 Determination of VMA and HVA in urine samples.

Reference

Chemicals and reagents

Phloroglucinol was obtained from Macklin Chemical Co., Ltd. (Shanghai, China). Choline chloride, Phenylephrine hydrochloride, formic acid (HPLC grade), acetic acid (HPLC grade), vanillylmandelic acid (VMA), homovanillic acid (HVA), β -estradiol, florfenicol, thiamphenicol, sodium sulfadimethoxine were obtained from Aladdin Chemical Co., Ltd. (Shanghai, China). Hexamethylenetetramine was obtained from Huadong Chemical Co., Ltd. (Tianjin, China). 1,4-butanediol was purchased from Guangfu Chemical Co., Ltd. (Tianjin, China). Acetonitrile and methanol were obtained from Xingke Biochem Co., Ltd. (Shanghai, China).

Characterization and analysis instruments

The characterization of the morphology of HIR and HNIR using scanning electron microscopy (SEM) with Phenom Pro SEM system (Phenom Pro Phenom, Netherlands).

Infrared spectra (IR) were recorded on a FTIR-850 fourier transform infrared spectrometer (Gangdong, China) in the range 500–4000 cm^{-1} . Hydrophilic properties were obtained by water contact angle system (SZ-CAMB3, Xuanzhun, China). The specific surface area of HIR was measured by a TriStar II 3020 automated pore size and surface area analyzer (Micromeritics, Norcross, USA). The chromatographic analysis was performed using VanquishTM Core HPLC system (Thermo Fisher Scientific, USA) with Accucore C₁₈ column (2.6 μm , 4.6 mm \times 100 mm, Thermo Fisher Scientific Co., Ltd). The mobile phase was water–acetonitrile (90:10, v/v, containing 0.1% formic acid in water) at a flow rate of 1.0 mL min^{-1} . The wavelengths of the UV set at 206 nm. The injection volume of the sample was 20 μL .

Adsorption experiments

3 mg HIR was placed in different 10 mL centrifuge tubes with 2 mL of VMA and HVA mixed standard solution ($40 \mu\text{g mL}^{-1}$). The tubes were placed in an oscillator shaking for 720 min at $25 \text{ }^\circ\text{C}$ and 300 rpm. After centrifugation, the supernatant was taken and passed through a $0.22 \mu\text{m}$ filter for HPLC analysis to determine the adsorption amounts of the HIR. The adsorption capacity (Q_e) of HIR to VMA and HVA was calculated by the following equation (1):¹

$$Q_e = \frac{(C_i - C_e) \times V}{W} \quad (1)$$

Where Q_e ($\mu\text{g mg}^{-1}$) represents the adsorption amount of HIR, C_i ($\mu\text{g mL}^{-1}$) is the initial concentration of VMA and HVA, C_e ($\mu\text{g mL}^{-1}$) represents the concentration of VMA and HVA after reaching adsorption equilibrium, V (mL) is the volume of the solution, W (mg) is the amount of HIR.

Adsorption kinetics

3 mg HIR and HNIR was placed in different 10 mL centrifuge tubes with 2 mL of VMA and HVA mixed standard solution ($40 \mu\text{g mL}^{-1}$). The tube was placed in an oscillator and the adsorption time ranged from 0.5 min to 720 min at $25 \text{ }^\circ\text{C}$ and 300 rpm. After centrifugation, the supernatant was taken and passed through a $0.22 \mu\text{m}$ filter for HPLC analysis. The adsorption amounts of the HIR and HNIR was calculated as Eq. (1).

The adsorption kinetics data of HIR was fitted by pseudo-first-order kinetic model and pseudo-second-order kinetic model, and the adsorption mechanism of HIR was studied with Eq. (2) and Eq. (3), respectively.²

$$\ln(Q_e - Q_t) = \ln Q_e - k_1 t \quad (2)$$

$$\frac{t}{Q_t} = \frac{t}{Q_e} + \frac{1}{k_2 Q_e^2} \quad (3)$$

Where Q_t ($\mu\text{g mg}^{-1}$) represents the amount of adsorption at time t , and Q_e ($\mu\text{g mg}^{-1}$) represents the amount of adsorption at adsorption equilibrium. k_1 (min^{-1}) is the Lagergren pseudo-first-order rate constant of adsorption and k_2 ($\text{g mg}^{-1} \text{min}^{-1}$) is the pseudo-second-order rate constant of adsorption. The results for the HIR and HNIR were shown in Fig. S2 and S3, Table S1 and S2.

Adsorption isotherms

HIR and HNIR (3 mg) was placed in different 10 mL centrifuge tubes, and 2 mL VMA and HVA mixed standard solution was added to the tubes at concentrations ranged from $2 \mu\text{g mL}^{-1}$ to $100 \mu\text{g mL}^{-1}$. Then put the tubes into an oscillator under 300 rpm at 298 K, 308 K, 318 K for 720 min. The supernatant was taken and passed through a $0.22 \mu\text{m}$ filter for HPLC analysis. The adsorption amounts of the HIR and HNIR were calculated as Eq. (1). The adsorption mechanism of HIR was analyzed using adsorption isotherms (Langmuir, Freundlich, Tempkin, and Dubin Radushkevich (D-R)) to investigate the adsorption process and mechanism of VMA and HVA on HIR.

The Langmuir adsorption model assumes that the surface of HIR contains uniform binding sites, and the adsorption of VMA and HVA by HIR is monolayer adsorption, and there is no interaction between the VMA and HVA. The linear equation of Langmuir's adsorption equation is shown in Eq. (4):³

$$\frac{C_e}{Q_e} = \frac{C_e}{Q_m} + \frac{1}{K_l Q_m} \quad (4)$$

Where Q_e ($\mu\text{g mg}^{-1}$) is the adsorption capacity of HIR or HNIR when the adsorption equilibrium is reached, and C_e ($\mu\text{g mL}^{-1}$) is the equilibrium concentration of VMA and HVA. Q_m ($\mu\text{g mg}^{-1}$) is the monomolecular layer saturation adsorption capacity of VMA and HVA. K_l ($\text{mL } \mu\text{g}^{-1}$) is the Langmuir adsorption equilibrium constant.

The Freundlich adsorption model describes that HIR's adsorption of VMA and HVA occurs on their heterogeneous surfaces and belongs to multimolecular layer adsorption. The adsorption capacity of VMA and HVA by HIR increases with the increase of their concentration. The linear equation of the Freundlich adsorption equation is shown in Eq. (5):⁴

$$\ln Q_e = \ln K_f + \frac{1}{n} \ln C_e \quad (5)$$

Where Q_e ($\mu\text{g mg}^{-1}$) is the adsorption capacity of HIR and HNIR when the adsorption equilibrium is reached, and C_e ($\mu\text{g mL}^{-1}$) is the equilibrium concentration of VMA and HVA. n and K_f are Freundlich constants related to the adsorption strength and capacity of HIR, respectively. n indicates the adsorption process of VMA and HVA by HIR, and the favorable adsorption condition is when $n > 1$.

The Tempkin isotherm model assumes a linear decrease in the adsorption heat of VMA and HVA in the adsorption layer of HIR, rather than a logarithmic decrease. The linear equation of the Tempkin adsorption equation is shown in Eq. (6):⁵

$$Q_e = B_T \ln A_T + B_T \ln C_e \quad (6)$$

Where Q_e ($\mu\text{g mg}^{-1}$) is the adsorption capacity of HIR and HNIR when the adsorption

equilibrium is reached, and C_e ($\mu\text{g mL}^{-1}$) is the equilibrium concentration of VMA and HVA. A_T (mL mg^{-1}) is the Tempkin isotherm constant related to the maximum binding energy, $B_T=R_T/b$, where R represents the gas constant with a value of 8.314 ($\text{J mol}^{-1} \text{K}^{-1}$), T represents the absolute temperature (K), and b is the Tempkin constant (J mol^{-1}), which is related to the adsorption heat.

The D-R model is used to study whether the adsorption process of HIR for VMA and HVA is physical or chemical adsorption, assuming that HIR does not have a uniform surface and a constant adsorption energy. The linear equation of the D-R adsorption equation are shown in Eq. (7), (8) and (9):⁶

$$\ln Q_e = \ln Q_m - \beta \varepsilon^2 \quad (7)$$

$$\varepsilon = RT \ln \left(1 + \frac{1}{C_e} \right) \quad (8)$$

$$E = (2\beta)^{-0.5} \quad (9)$$

Where Q_e ($\mu\text{g mg}^{-1}$) is the adsorption capacity of HIR and HNIR when the adsorption equilibrium is reached, and C_e ($\mu\text{g mL}^{-1}$) is the equilibrium concentration of VMA and HVA, Q_m ($\mu\text{g mg}^{-1}$) represents the maximum adsorption capacity. β is the constant related to the adsorption energy ($\text{mol}^2 \text{J}^{-2}$) and ε is the Polanyi potential. E (kJ mol^{-1}) is the average energy that can be calculated from Eq. (9). The value of E indicates whether the adsorption process of HIR is chemical or physical adsorption. $E > 8 \text{ kJ mol}^{-1}$ indicates that the adsorption process of HIR is chemical adsorption, while $E < 8 \text{ kJ mol}^{-1}$ indicates that the adsorption process of HIR is physical reaction.

The adsorption process and mechanism of prepared HIR on VMA and HVA can be studied by thermodynamic analysis. The main thermodynamic parameters are enthalpy

change (ΔH), entropy change (ΔS) and Gibbs free energy (ΔG), and the relevant calculation equations are as follows:⁷

$$K_c = Q_e / C_e \quad (10)$$

$$\ln K_c = -\frac{\Delta H}{RT} + \frac{\Delta S}{R} \quad (11)$$

$$\Delta G = \Delta H - T \Delta S \quad (12)$$

Where Q_e ($\mu\text{g mg}^{-1}$) is the adsorption capacity of HIR and HNIR when the adsorption equilibrium is reached, and C_e ($\mu\text{g mL}^{-1}$) is the equilibrium concentration of VMA and HVA. T is the system temperature, R represents the gas constant with a value of 8.314 ($\text{J mol}^{-1} \text{K}^{-1}$).

Urine sample pretreatment procedure

Urine samples from 10 healthy volunteers (4 females and 6 males) aged 20-30 years were collected for analysis. After the urine sample was repeatedly frozen and thawed for several times, the supernatant was obtained by high-speed centrifugation (10000 rpm for 10 min) and then the supernatant was taken and passed through a 0.22 μm filter. The urine was then diluted to 10 times its original volume with water.

Figures and Tables

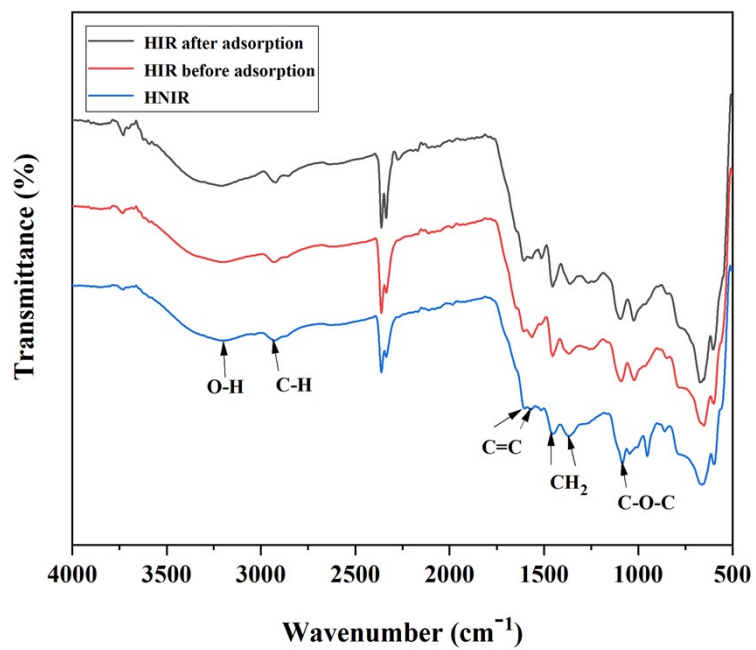


Fig. S1 Fourier-transform infrared spectroscopy (FTIR) spectra of HIR and HNIR.

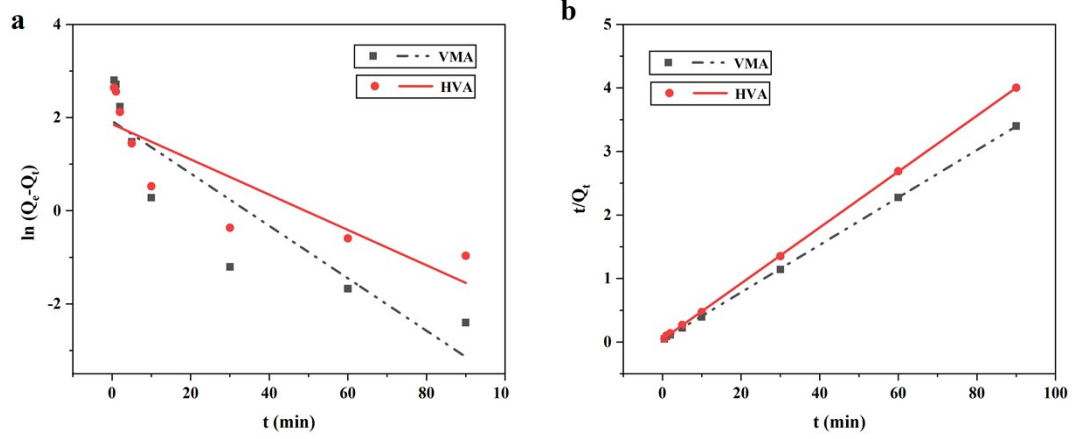


Fig. S2 Pseudo-first-order (a) and Pseudo-second-order (b) kinetics models of HIR for adsorption of VMA and HVA.

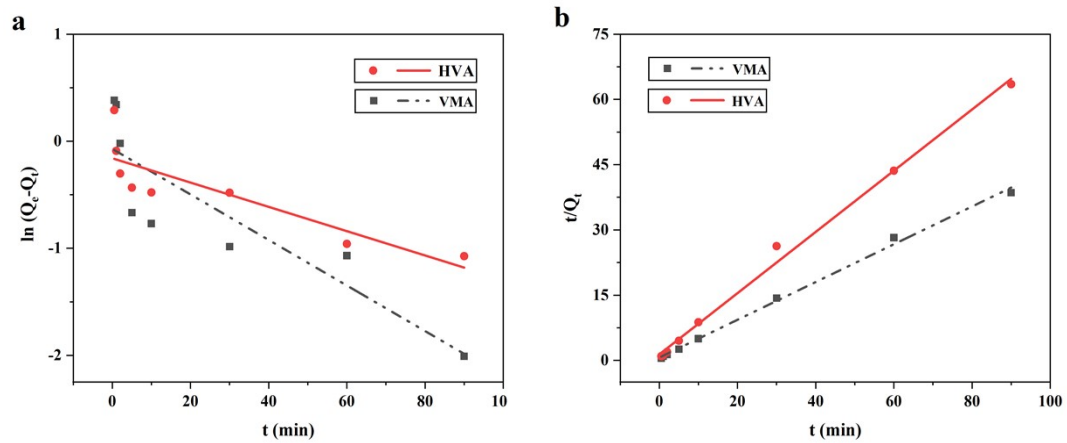


Fig. S3 Pseudo-first-order (a) and Pseudo-second-order (b) kinetics models of HNIR for adsorption of VMA and HVA.

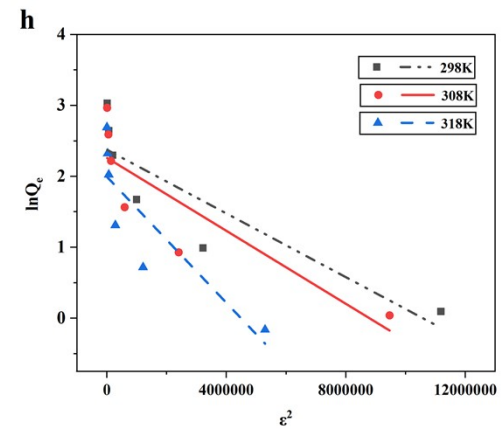
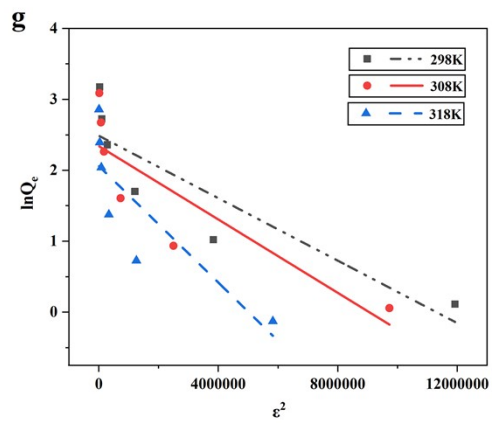
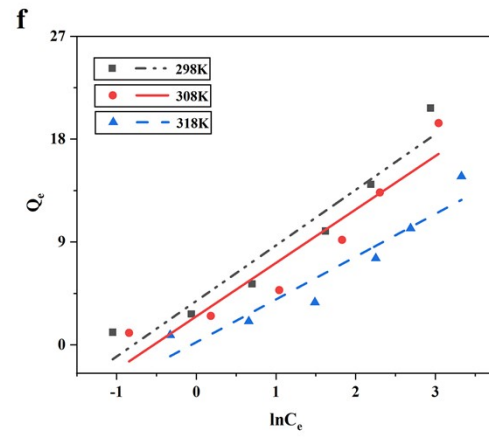
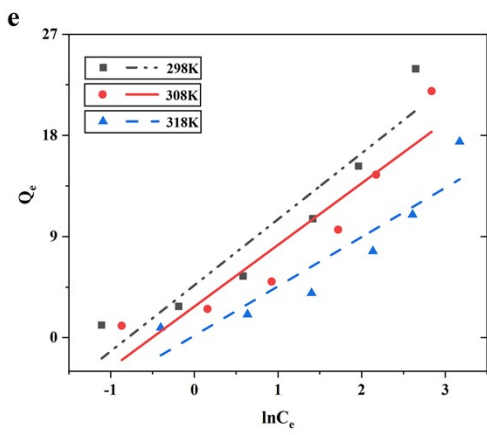
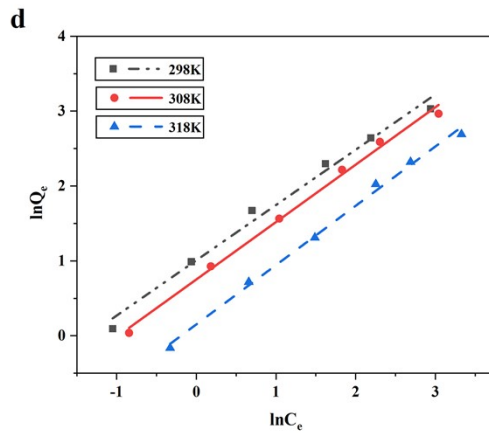
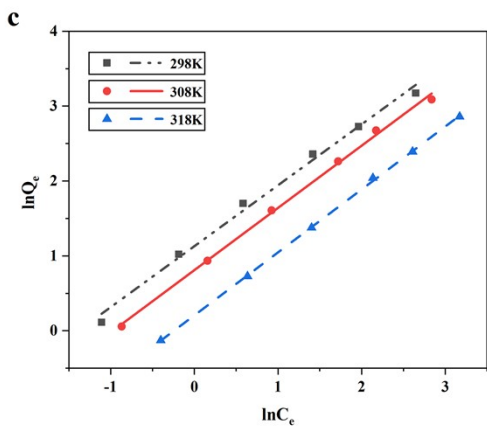
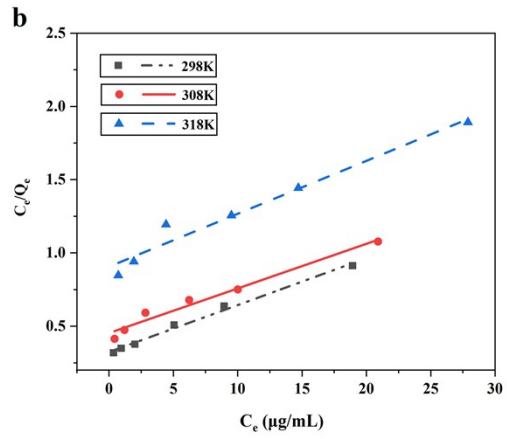
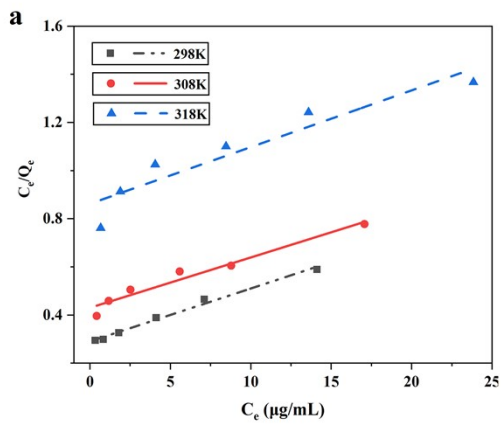


Fig. S4 Adsorption isotherm models of HIR for adsorption of VMA and HVA at different temperatures. (a) Langmuir linear fits for VMA; (b) Langmuir linear fits for HVA; (c) Freundlich linear fits for VMA; (d) Freundlich linear fits for HVA; (e) Tempkin linear fits for VMA; (f) Tempkin linear fits for HVA; (g) D-R linear fits for VMA; (h) D-R linear fits for HVA.

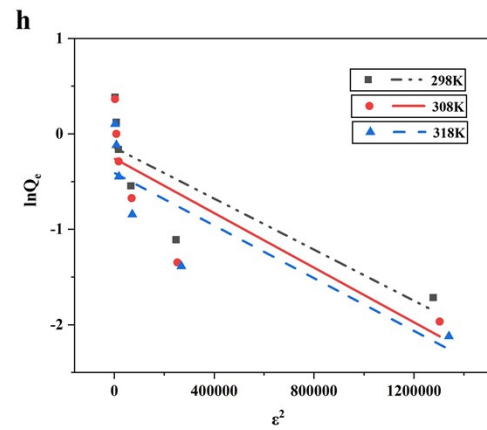
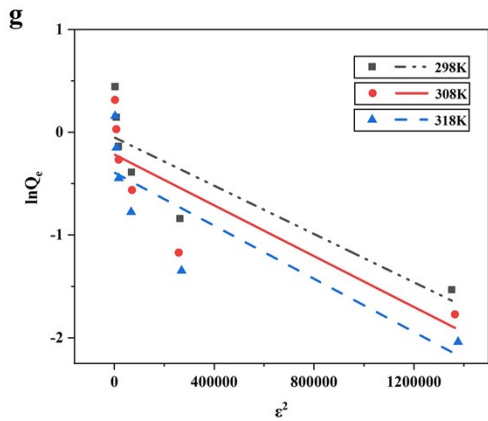
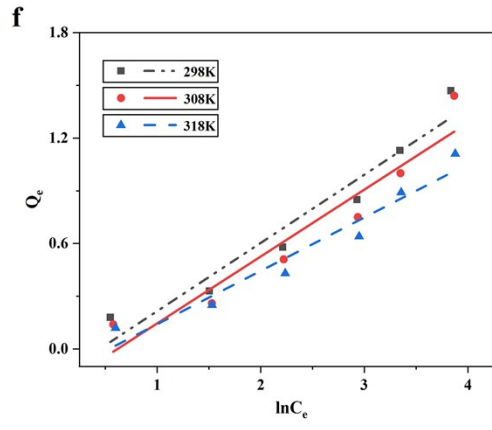
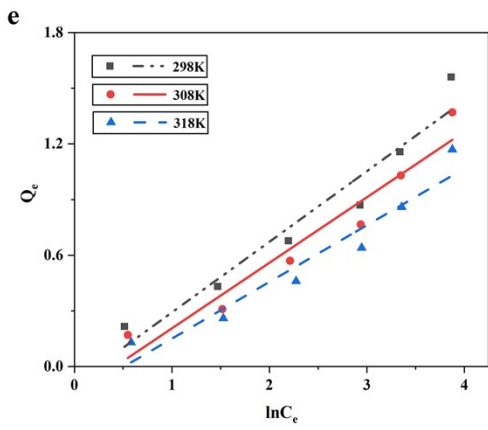
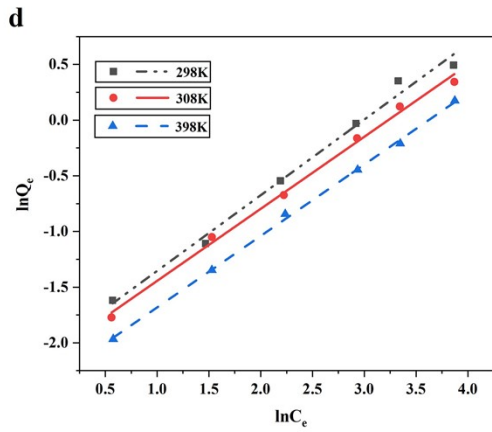
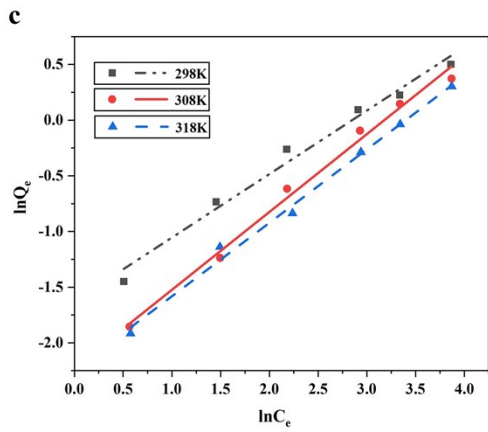
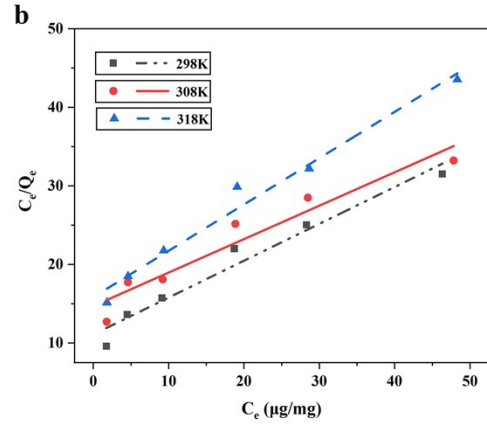
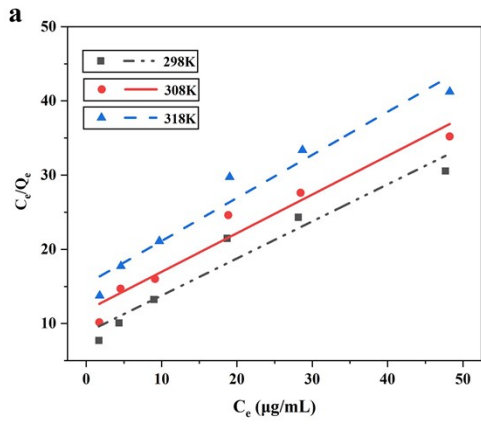


Fig. S5 Adsorption isotherm models of HNIR for adsorption of VMA and HVA at different temperatures. (a) Langmuir linear fits for VMA; (b) Langmuir linear fits for HVA; (c) Freundlich linear fits for VMA; (d) Freundlich linear fits for HVA; (e) Tempkin linear fits for VMA; (f) Tempkin linear fits for HVA; (g) D-R linear fits for VMA; (h) D-R linear fits for HVA.

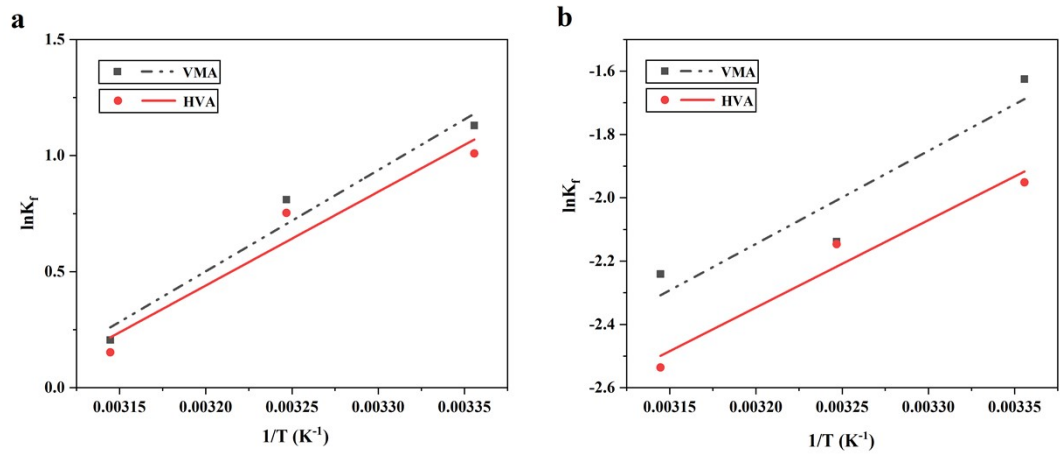


Fig. S6 The plots of $\ln K_f$ versus $1/T$ for VMA and HVA of HIR (a) and HNIR (b).

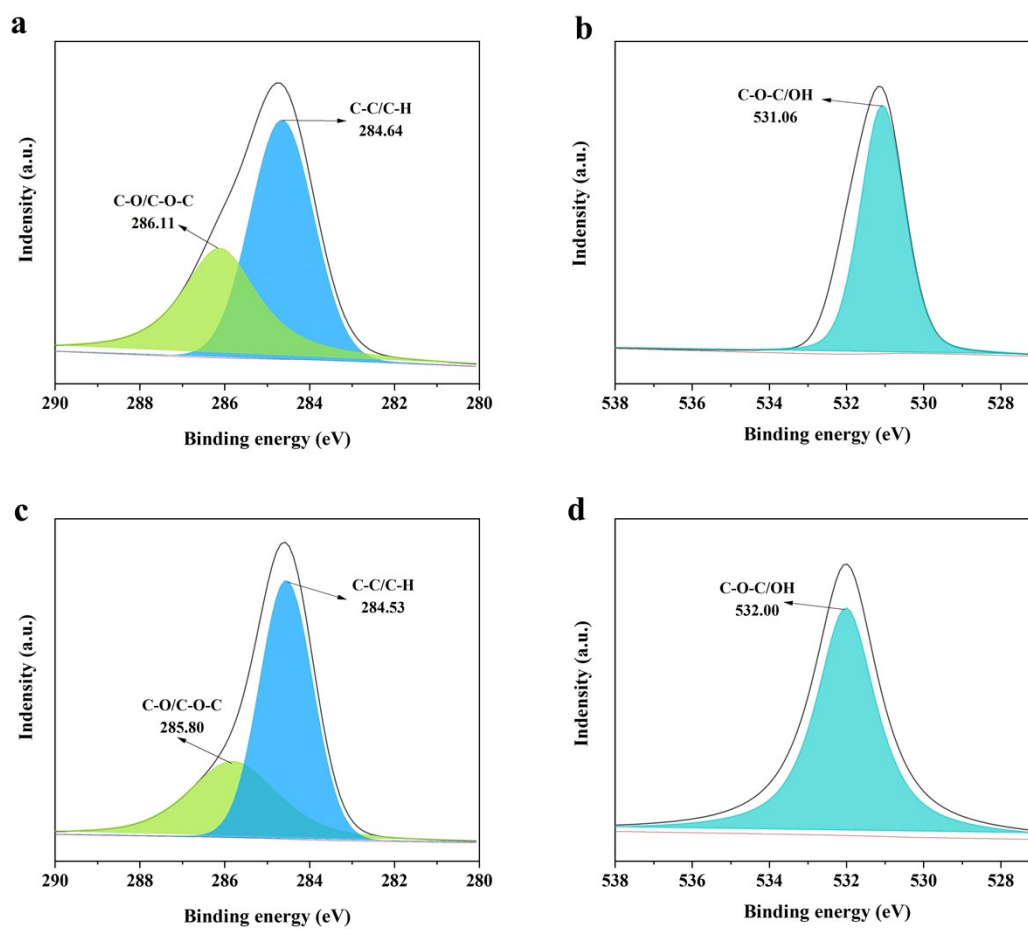


Fig. S7 High-resolution XPS spectra of HIR before adsorption of VMA, HVA (a) C1s, (b) O1s and after adsorption of VMA, HVA (c) C1s, (d) O1s.

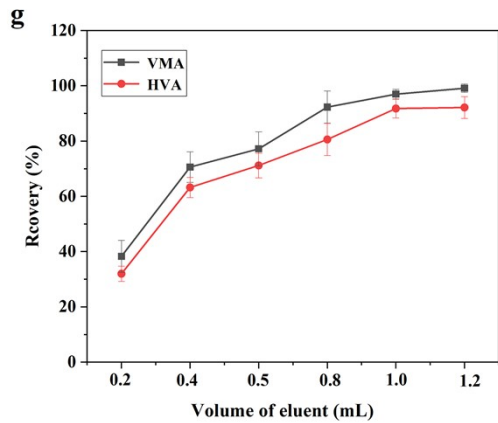
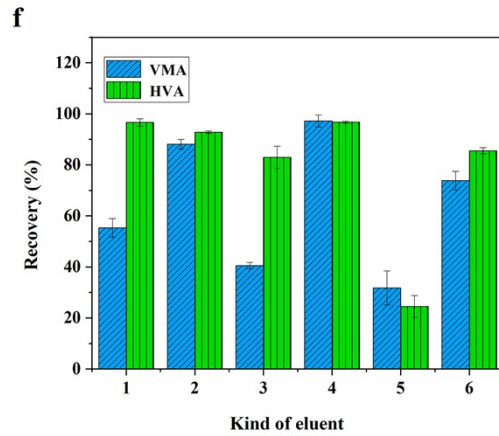
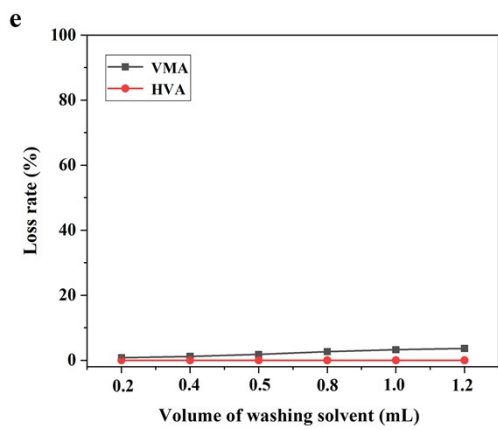
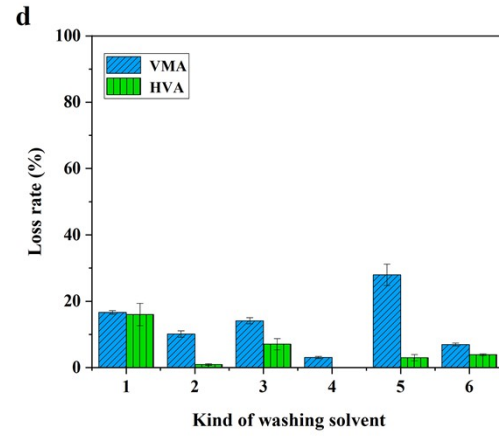
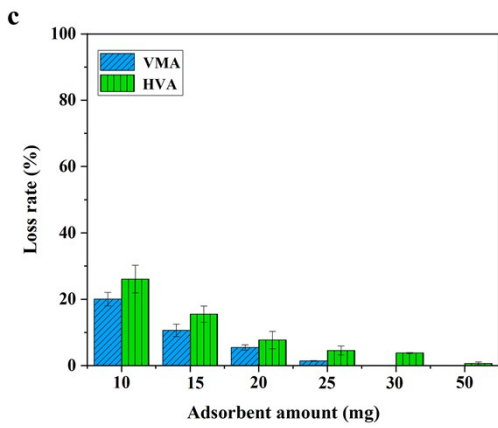
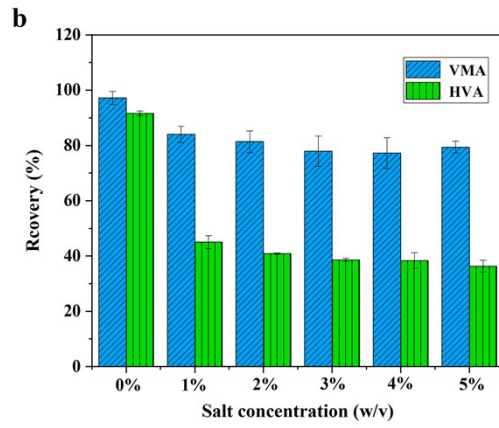
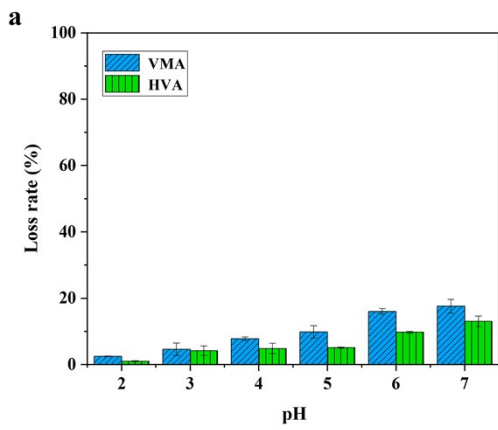


Fig. S8 Effect factors of separation and extraction conditions study. (a) pH; (b) salt concentration; (c) adsorbent amount; (d) the kind of washing solvent (1.methanol; 2.acetonitrile; 3.acetone; 4.water; 5.methanol-water (1:1, v/v); 6.acetonitrile-water (1:1, v/v)); (e) the volume of washing solvent; (f) the kind of eluent (1.methanol-acetic acid (9:1, v/v); 2.methanol-formic acid (9:1, v/v); 3.acetonitrile-acetic acid (9:1, v/v); 4.acetonitrile-formic acid (9:1, v/v); 5.acetonitrile-ammonia water (9:1, v/v); 6.methanol-ammonia water (9:1, v/v)); (g) the volume of eluent).

Table S1 Lagergren pseudo-first-order and pseudo-second-order kinetics parameters of HIR for

the adsorption of VMA and HVA

Analyte	Pesudo-first-order			Pesudo-second-order		
	k_1 (min ⁻¹)	Q_e (μg mg ⁻¹)	R ²	k_2 (min ⁻¹)	Q_e (μg mg ⁻¹)	R ²
VMA	0.0563	6.8689	0.7848	0.0340	28.7935	0.9999
HVA	0.0379	6.4408	0.7034	0.0571	20.0468	0.9999

Table S2 Lagergren pseudo-first-order and pseudo-second-order kinetics parameters of HNIR for the adsorption of VMA and HVA

Analyte	Pseudo-first-order			Pseudo-second-order		
	k_1 (min ⁻¹)	Q_e (μg mg ⁻¹)	R ²	k_2 (min ⁻¹)	Q_e (μg mg ⁻¹)	R ²
VMA	0.0213	0.9329	0.7324	0.2912	2.3026	0.9945
HVA	0.0114	0.8528	0.7028	0.0688	3.2469	0.9965

Table S3 Langmuir isotherm for the adsorption of analytes on HIR

T (K)	Analyte	Langmuir constants		
		K_l (mL μg^{-1})	Q_e (mg g^{-1})	R^2
298 K	VMA	0.0756	45.4959	0.9867
	HVA	0.0989	31.2109	0.9908
308 K	VMA	0.0485	47.8469	0.9492
	HVA	0.0671	32.8407	0.9679
318 K	VMA	0.0273	42.4268	0.8624
	HVA	0.0398	27.6931	0.9554

Table S4 Langmuir isotherm for the adsorption of analytes on HNIR

T (K)	Analyte	Langmuir constants		
		K_l (mL μg^{-1})	Q_e (mg g^{-1})	R^2
298 K	VMA	0.0568	2.0021	0.9314
	HVA	0.0422	2.1330	0.9527
308 K	VMA	0.0442	1.9201	0.9434
	HVA	0.0289	2.3513	0.9112
318 K	VMA	0.0378	1.7237	0.9435
	HVA	0.0371	1.6977	0.9733

Table S5 Freundlich isotherm for the adsorption of analytes on HIR

T (K)	Analyte	Freundlich constants		
		$K_f(\text{mg g}^{-1})$	n	R^2
298 K	VMA	3.0953	1.2287	0.9919
	HVA	2.7429	1.3546	0.9894
308 K	VMA	2.2483	1.2032	0.9976
	HVA	2.1239	1.3048	0.9940
318 K	VMA	1.2289	1.1893	0.9996
	HVA	1.1652	1.2631	0.9948

Table S6 Freundlich isotherm for the adsorption of analytes on HNIR

T (K)	Analyte	Freundlich constants		
		$K_f(\text{mg g}^{-1})$	n	R^2
298 K	VMA	0.1969	1.7533	0.9832
	HVA	0.1202	1.4712	0.9910
308 K	VMA	0.1178	1.4296	0.9918
	HVA	0.1169	1.5453	0.9957
318 K	VMA	0.1064	1.5157	0.9933
	HVA	0.0792	1.5583	0.9988

Table S7 Tempkin isotherm for the adsorption of analytes on HIR

T (K)	Analyte	Tempkin constants		
		A_T	B_T	R ²
298 K	VMA	2.2096	5.8753	0.8775
	HVA	2.2014	4.8623	0.9108
308 K	VMA	1.6550	5.4868	0.8496
	HVA	1.7044	4.6755	0.8776
318 K	VMA	1.0416	4.3866	0.8239
	HVA	1.0625	3.7425	0.8803

Table S8 Tempkin isotherm for the adsorption of analytes on HNIR

T (K)	Analyte	Tempkin constants		
		A_T	B_T	R ²
298 K	VMA	0.7924	0.3805	0.9221
	HVA	0.6376	0.3879	0.9229
308 K	VMA	0.6591	0.3531	0.9222
	HVA	0.5329	0.3804	0.8917
318 K	VMA	0.6018	0.3056	0.9141
	HVA	0.5848	0.3036	0.9323

Table S9 D-R isotherm for the adsorption of analytes on HIR

T (K)	Analyte	D-R constants		
		Q_e (mg g ⁻¹)	E (kJ mol ⁻¹)	R ²
298 K	VMA	12.0480	1.5073	0.7555
	HVA	10.7743	1.4923	0.7448
308 K	VMA	10.4174	1.3905	0.6865
	HVA	9.6128	1.3555	0.6958
318 K	VMA	7.8744	1.1033	0.6424
	HVA	7.3672	1.0611	0.6760

Table S10 D-R isotherm for the adsorption of analytes on HNIR

T (K)	Analyte	D-R constants		
		Q_e (mg g ⁻¹)	E (kJ mol ⁻¹)	R ²
298 K	VMA	0.9511	0.65243	0.7046
	HVA	0.8663	0.6222	0.6494
308 K	VMA	0.8050	0.6362	0.6544
	HVA	0.7729	0.5913	0.6321
318 K	VMA	0.6756	0.6221	0.6797
	HVA	0.6646	0.6021	0.6926

Table S11 Thermodynamics parameters for the adsorption of analytes on HIR

Analyte	ΔH (kJ mol ⁻¹)	ΔS (J mol ⁻¹ K ⁻¹)	ΔG (kJ mol ⁻¹)			R ²
			298K	308K	318K	
VMA	-36.2562	-0.1108	-3.2229	-2.1141	-1.0059	0.9252
HVA	-33.5668	-0.1037	-2.6487	-1.6114	-0.5736	0.8804

Table S12 Thermodynamics parameters for the adsorption of analytes on HNIR

Analyte	ΔH (kJ mol ⁻¹)	ΔS (J mol ⁻¹ K ⁻¹)	ΔG (kJ mol ⁻¹)			R ²
			298K	308K	318K	
VMA	-24.4132	-0.0670	-4.4472	-3.7772	-3.1072	0.8825
HVA	-27.7819	-0.0772	-4.7763	-4.0043	-3.2323	0.9572

Analytes	Regression equation	r	Linearity	LOD	LOQ	RSD (%)	
			($\mu\text{g mL}^{-1}$)	(ng mL^{-1})	(ng mL^{-1})	Intra-day	Inter-day
VMA	$y=1.1389x+0.0094$	0.9999	0.05-150	0.5	1.5	2.5	2.9
HVA	$y=1.0387x+0.0063$	0.9999	0.05-150	1.0	3.5	1.4	1.7

Table S13 Methodology parameters of the HIR-SPE-HPLC

Table S14 Spiked recovery of the HIR-SPE-HPLC method

Analytes	2.0 ($\mu\text{g mL}^{-1}$)		10.0 ($\mu\text{g mL}^{-1}$)		100.0 ($\mu\text{g mL}^{-1}$)	
	Recovery (%)	RSD (%)	Recovery (%)	RSD (%)	Recovery (%)	RSD (%)
VMA	111.3	7.8	101.4	4.1	90.7	3.2
HVA	108.2	5.3	92.6	4.9	93.8	4.9

Table S15 Determination of VMA and HVA in urine samples

Sample	VMA ($\mu\text{g mL}^{-1}$)	HVA ($\mu\text{g mL}^{-1}$)
1	0.62 ± 0.08	1.47 ± 0.08
2	0.71 ± 0.07	2.55 ± 0.08
3	0.17 ± 0.04	0.91 ± 0.13
4	0.88 ± 0.08	0.63 ± 0.05
5	0.28 ± 0.03	1.25 ± 0.11
6	0.44 ± 0.07	1.85 ± 0.15
7	0.59 ± 0.03	1.92 ± 0.12
8	0.38 ± 0.03	2.09 ± 0.09
9	0.54 ± 0.04	2.56 ± 0.06
10	1.42 ± 0.11	1.52 ± 0.14

Reference

- 1 X. Zhong, Z. Lu, W. Liang and B. Hu, *J. Hazard. Mater.*, 2020, **393**, 122353.
- 2 X. Xie, X. Ma, L. Guo, Y. Fan, G. Zeng, M. Zhang and J. Li, *Chem. Eng. J.*, 2019, **357**, 56–65.
- 3 L. Wang, J. Li, J. Wang, X. Guo, X. Wang, J. Choo and L. Chen, *J. Colloid Interface Sci.*, 2019, **541**, 376–386.
- 4 A. Grover, I. Mohiuddin, A. K. Malik, J. S. Aulakh and K. H. Kim, *J. Cleaner Prod.*, 2019, **240**, 118090.
- 5 Q. Song, J. Liang, Y. Fang, C. Cao, Z. Liu, L. Li, Y. Huang, J. Lin and C. Tang, *J. Hazard. Mater.*, 2019, **364**, 654–662.
- 6 A. K. Priya, V. Yogeshwaran, S. Rajendran, T. K. A. Hoang, M. Soto-Moscoso, A. A. Ghfar and C. Bathula, *Chemosphere*, 2022, **286**, 131796.
- 7 F. Karimi, A. Ayati, B. Tanhaei, A. L. Sanati, S. Afshar, A. Kardan, Z. Dabirifar and C. Karaman, *Environ. Res.*, 2022, **203**, 111753.